Hindawi
Mathematical Problems in Engineering
Volume 2021, Article ID 8883752, 10 pages
https://doi.org/10.1155/2021/8883752

Research Article

Fault-Tolerant Control for *N*-Link Robot Manipulator via Adaptive Nonsingular Terminal Sliding Mode Control Technology

Nannan Shi,[1] Fanghui Luo,[1] Zhikuan Kang,[1] Lihui Wang,[1] Zhuo Zhao,[1] Qiang Meng ,[2,3] and Weiqin Hou[2,3]

[1]*Seismic Engineering and Structure Key Laboratory of Beijing, Beijing University of Technology, Beijing 100124, China*
[2]*Guangdong RULEBIT Intelligent Robot Technology Co., Ltd., Zhuhai 519000, China*
[3]*Shenzhen RULEBIT Intelligent Robot Technology Co., Ltd., Shenzhen 518000, China*

Correspondence should be addressed to Qiang Meng; qiang.meng@rulebittech.com

Received 24 September 2020; Revised 19 May 2021; Accepted 22 June 2021; Published 6 July 2021

Academic Editor: Shihong Ding

An adaptive nonsingular terminal sliding mode control (ANTSMC) scheme for the *n*-link robot manipulator is presented in this study, which can achieve faster convergence and higher precision tracking compared with the linear hyperplane-based sliding mode control. Novel adaptive updating laws based on the actual tracking error are employed to online adjust the upper bound of uncertainty, which comprehensively consider both the tracking performance and chattering eliminating problem. The stability analysis of the proposed ANTSMC is verified using the Lyapunov method with the existence of the parameter uncertainty and the actuator faults. Numerical simulation studies the comparison of performance between ANTSMC and the conventional nonsingular terminal sliding mode control (NTSMC) scheme to validate the advantages of the proposed control algorithm.

1. Introduction

Robot manipulators play a pivotal role in the modern industrial field, whose dynamics are typically multi-input multioutput (MIMO) nonlinear systems. In practice, parameter variations and external disturbances are inevitable for the mechanical systems. Moreover, high accuracy and safety demands of the robot manipulator cause a greatly increasing attention to the unpredictable faults. Recently, many fault detection methods have been successfully employed for the robot manipulators [1–6], such as the prediction-error-based approach [1], second-order sliding mode observer [2, 3], nonlinear observer [4], optimal unknown input observer [6], and power consumption modeling based method [5]. Besides, the fault-tolerant control research applied in the robot manipulators has been a hot topic. Song introduced a multilayered feed-forward neural network to identify the faults for robot manipulator and then achieved the tracking performance in the presence of uncertainty [7]. Siqueira et al. [8] proposed an output-feedback H_∞ fault-tolerant controller for robot manipulators by linearizing the dynamic model around the operation point. In 2009, Siqueira and Terra [9] further derived H_2, H_∞, and mixed H_2/H_∞ Markovian algorithms for the robot manipulator, but their drawbacks are still the linearization problems. Liu et al. [10] published a novel robust fixed-time fault-tolerant tracking controller for the uncertain robot manipulator. Hagh et al. [11] gave an active fault-tolerant control design for actuator fault mitigation in robotic manipulators. In this paper, we aim to develop a simple and effective passive fault-tolerant control algorithm for the robot manipulator without the fault detection and diagnosis (FDD) module.

Sliding mode control (SMC) schemes are well known for their robustness to the parameter variation and disturbances and have been successfully adopted in many nonlinear systems [12–16]. To assure the finite-time convergence, the terminal sliding mode control (TSMC) has been derived to reach the equilibrium point within a finite time to realize high accuracy control [17]. Besides, the singularity problem of the conventional TSMC has been overcome by indirect [17, 18] and direct approaches [19]. Nowadays, researchers

focus on the unknown functions estimated or designed for the TSMC. Since neural networks and fuzzy logic are universal function approximations, the mixed control algorithms combining them and the TSMC technologies have been extensively employed. Lin proposed an adaptive nonsingular TSMC method for the robotic systems using fuzzy wavelet networks and verified the corresponding controller on a six-link robot manipulator [20]. A dynamics estimation method based on an adaptive algorithm and fuzzy logic is introduced to the nonsingular TSMC for a class of MIMO uncertain nonlinear systems [21]. Xu et al. derived a TSMC based on adaptive fuzzy-neural observer for nonaffine nonlinear system [22]. Cao et al. also used the adaptive fuzzy algorithm to achieve an adaptive nonsingular TSMC for the fault-tolerant small satellite attitude control [23]. Moreover, other adaptive TSMC schemes using different adaptive updating laws without the neural networks and fuzzy logic have also been successfully adopted in many nonlinear systems, such as the electromechanical actuator [24], spacecraft formation flying [25], uncertain nonlinear single-input single-output (SISO) systems [26], and nonlinear differential inclusion systems [27]. However, for the robot manipulator, only the nonsingular TSMC control schemes have been developed [18, 28], though the upper bound of the uncertainty is usually unknown in most of the real systems (especially in the faulty conditions). In fact, the upper bound uncertainty of the nonsingular TSMC for the robot manipulator is conventionally designed as a fixed one, which will bring a trade-off problem between the control accuracy and the control chattering. Therefore, we hope to derive a novel adaptive nonsingular TSMC for the robot manipulator by combining an adaptive updating law to consider both the control accuracy and the control chattering.

Motivated by the above discussion, an adaptive nonsingular TSMC scheme for the robot manipulators with the existence of the parameter uncertainty and the actuator faults is derived in this paper, which can online tune the upper bound of the uncertainty to ensure the high precise tracking performance, finite time convergence, and Lyapunov stability.

2. Problem Formulation

The n-link robot manipulator dynamics can be formulated as

$$\mathbf{M}(\mathbf{q})\ddot{q} + \mathbf{C}(\mathbf{q}, \dot{q}) + \mathbf{G}(\mathbf{q}) = \boldsymbol{\tau}, \tag{1}$$

where $\mathbf{M}(\mathbf{q})$, $\mathbf{C}(\mathbf{q}, \dot{q})$, and $\mathbf{G}(\mathbf{q})$ denote the inertia matrix, Coriolis and centrifugal forces, and gravitational torque, respectively, $\mathbf{q}$ represents the generalized coordinates, and τ is the joint torque.

Considering the uncertainties and actuator faults, the dynamics of the uncertain robot manipulator can be rewritten as

$$(\mathbf{M}_0 + \Delta\mathbf{M})\ddot{q} + (\mathbf{C}_0 + \Delta\mathbf{C}) + (\mathbf{G}_0 + \Delta\mathbf{G}) = \boldsymbol{\delta}_a(\boldsymbol{\tau} + \boldsymbol{\delta}_f), \tag{2}$$

where $\mathbf{M}_0$, $\mathbf{C}_0$, and $\mathbf{G}_0$ represent the estimated terms; $\Delta\mathbf{M}$, $\Delta\mathbf{C}$, and $\Delta\mathbf{G}$ denote the uncertain terms; δ_a and δ_f are the multiplicative and additive faults.

Equation (2) can be further rearranged as

$$\mathbf{M}_0\ddot{q} + \mathbf{C}_0 + \mathbf{G}_0 = \boldsymbol{\tau} + \boldsymbol{\delta}_{\text{total}}, \tag{3}$$

$$\begin{aligned}\boldsymbol{\delta}_{\text{total}} = &\left(\boldsymbol{\delta}_a(\boldsymbol{\tau} + \boldsymbol{\delta}_f) - \boldsymbol{\tau}\right) \\ &- \Delta\mathbf{G} - \Delta\mathbf{C} - \Delta\mathbf{M}\ddot{q}\end{aligned}, \tag{4}$$

where δ_{total} denotes the total uncertainty of the robot manipulator.

3. Nonsingular Terminal Sliding Mode Control (NTSMC)

In this section, the nonsingular terminal sliding mode control (NTSMC) proposed by Man and Yu [18] is briefly described, which solves the singular problem of the TSMC by direct approach.

Lemma 1 (see [18]). *For the uncertain n-link manipulator (described by equation (3)), if the NTSMC manifold and its input command are formulated by equations (5)–(8) and Assumption 1 holds, then the system tracking error ε will converge to zero in finite time.*

$$\mathbf{s} = \boldsymbol{\varepsilon} + \boldsymbol{\Lambda}\dot{\varepsilon}^{p/q}, \tag{5}$$

where

$$\begin{aligned}\boldsymbol{\tau}_{\text{ntsmc}} = &\mathbf{M}_0\ddot{q}_d + \mathbf{C}_0 \\ &+\mathbf{G}_0 - \frac{q}{p}\mathbf{M}_0\boldsymbol{\Lambda}^{-1}\dot{\varepsilon}^{2-(p/q)} - \frac{\left[\mathbf{s}^T\mathbf{W}\right]^T}{\left\|\mathbf{s}^T\mathbf{W}\right\|^2}\|\mathbf{s}\|\|\mathbf{W}\|\Gamma_{\text{constant}},\end{aligned} \tag{6}$$

$$\Gamma_{\text{constant}} = b_1 + b_2\|\mathbf{q}\| + b_3\|\dot{q}\|^2, \tag{7}$$

$$\mathbf{W} = \boldsymbol{\Lambda}\text{diag}\left(\dot{\varepsilon}^{(p/q)-1}\right)\mathbf{M}_0^{-1}, \tag{8}$$

where $\varepsilon = \mathbf{q} - \mathbf{q}_d$; $\mathbf{q}$ and $\mathbf{q}_d$ represent the actual input and desired input, respectively; p and q are positive odd integers, which satisfy $1 < p/q < 2$; and $\Lambda = diag[\lambda_1, \ldots, \lambda_n]$ denotes a design matrix.

Assumption 1. The total uncertainty δ_{total} of the robot manipulator can be bounded, which can be formulated as [18]

$$\left\|\boldsymbol{\delta}_{\text{total}}\right\| < b_1 + b_2\|\mathbf{q}\| + b_3\|\dot{q}\|^2, \tag{9}$$

where b_1, b_2, and b_3 are positive numbers.

Remark 1. Lemma 1 gives a conventional NTSMC scheme for the robot manipulator based on Assumption 1, and the design parameters (b_1, b_2, and b_3) of the upper bound Γ_{constant} are constant. In practice, the high upper bound can obtain the high-quality tracking performance at the cost of serious chattering, and the low upper bound owns the

opposite characteristic. Moreover, unpredictable faults may cause the great change of the uncertainty upper bound satisfying Assumption 1. Therefore, it is a hard task to choose an appropriate upper bound Γ_{constant} for the NTSMC.

4. Adaptive Nonsingular Terminal Sliding Mode Control

To appropriately select the uncertainty upper bound of the NTSMC, adaptive updating methods are natural choices. Considering the mechanical systems, there are some special stages: (1) in the start-up phase, the initial trajectory error causes the large starting torque, which appears to be serious chattering phenomenon for the SMC control schemes; (2) in the stability phase, the tracking performance is affected by the system uncertainty; and (3) in the faulty condition, the uncertainty of the nonlinear system may generate great change. Therefore, the uncertainty upper bound of the NTSMC should be chosen to be a low one, a moderate one, and a high one for the above three stages, respectively.

In this section, we introduce adaptive updating laws based on the tracking errors to online adjust the uncertainty upper bound, which are summarized as follows.

Theorem 1. *For the uncertain n-link robot manipulator (described by equation (3)), if the adaptive nonsingular terminal sliding mode control (ANTSMC) manifold and its input command are formulated by equations (10)–(16) and Assumption 1 holds, then the system tracking error ε will converge to zero in finite time.*

$$\mathbf{s} = \boldsymbol{\varepsilon} + \boldsymbol{\Lambda}\dot{\varepsilon}^{p/q}, \tag{10}$$

$$\begin{aligned}\boldsymbol{\tau}_{\text{antsmc}} = {} & \mathbf{M}_0\ddot{q}_d + \mathbf{C}_0 + \mathbf{G}_0 - \frac{q}{p}\mathbf{M}_0\boldsymbol{\Lambda}^{-1}\dot{\varepsilon}^{2-(p/q)} \\ & - \frac{\left[\mathbf{s}^T\mathbf{W}\right]^T}{\left\|\mathbf{s}^T\mathbf{W}\right\|^2}\|\mathbf{s}\|\|\mathbf{W}\|\widehat{\Gamma}_{\text{adaptive}},\end{aligned} \tag{11}$$

$$\mathbf{W} = \boldsymbol{\Lambda}\text{diag}\left(\dot{\varepsilon}^{(p/q)-1}\right)\mathbf{M}_0^{-1}. \tag{12}$$

Moreover, the updating laws are chosen as

$$\widehat{\Gamma}_{\text{adaptive}} = \widehat{b}_1 + \widehat{b}_2\|\mathbf{q}\| + \widehat{b}_3\|\dot{q}\|^2, \tag{13}$$

$$\dot{\widehat{b}}_1 = d_1 \cdot \frac{p}{q}\|\mathbf{W}\|\|\mathbf{s}\|, \tag{14}$$

$$\dot{\widehat{b}}_2 = d_2 \cdot \frac{p}{q}\|\mathbf{W}\|\|\mathbf{s}\|\|\mathbf{q}\|, \tag{15}$$

$$\dot{\widehat{b}}_3 = d_3 \cdot \frac{p}{q}\|\mathbf{W}\|\|\mathbf{s}\|\|\dot{q}\|^2, \tag{16}$$

where $\widehat{\Gamma}_{\text{adaptive}}$, $\widehat{b}_1$, $\widehat{b}_2$, and $\widehat{b}_3$ denote the adaptive estimated values and d_1, d_2, and d_3 are constants.

Proof. Consider the following Lyapunov function:

$$V_{\text{antsmc}} = \frac{1}{2}\left(s^T s + \frac{1}{d_1}\widetilde{b}_1^T\widetilde{b}_1 + \frac{1}{d_2}\widetilde{b}_2^T\widetilde{b}_2 + \frac{1}{d_3}\widetilde{b}_3^T\widetilde{b}_3\right), \tag{17}$$

where $\widetilde{b}_1$, $\widetilde{b}_2$, and $\widetilde{b}_3$ represent the mismatch between the actual and estimated parameters.

$$\widetilde{b}_1 = b_1 - \widehat{b}_1, \tag{18}$$

$$\widetilde{b}_2 = b_2 - \widehat{b}_2, \tag{19}$$

$$\widetilde{b}_3 = b_3 - \widehat{b}_3. \tag{20}$$

Differentiating V_{antsmc} with respect to time and substituting equation (10) and equations (18)–(20) into it yield

$$\dot{V}_{\text{antsmc}} = \mathbf{s}^T\left(\dot{\varepsilon} + \frac{p}{q}\boldsymbol{\Lambda}\text{diag}\left(\dot{\varepsilon}^{(p/q)-1}\right)\ddot{\varepsilon}\right) - \frac{1}{d_1}\widetilde{b}_1^T\dot{\widehat{b}}_1 - \frac{1}{d_2}\widetilde{b}_2^T\dot{\widehat{b}}_2 - \frac{1}{d_3}\widetilde{b}_3^T\dot{\widehat{b}}_3. \tag{21}$$

Substituting equation (3) into equation (21) gives

$$\dot{V}_{\text{antsmc}} = \mathbf{s}^T\left(\dot{\varepsilon} + \frac{p}{q}\boldsymbol{\Lambda}\text{diag}\left(\dot{\varepsilon}^{(p/q)-1}\right)\left(\mathbf{M}_0^{-1}\left(\boldsymbol{\tau}_{\text{antsmc}} + \boldsymbol{\delta}_{\text{total}} - \mathbf{C}_0 - \mathbf{G}_0\right) - \ddot{q}_d\right)\right) - \frac{1}{d_1}\widetilde{b}_1^T\dot{\widehat{b}}_1 - \frac{1}{d_2}\widetilde{b}_2^T\dot{\widehat{b}}_2 - \frac{1}{d_3}\widetilde{b}_3^T\dot{\widehat{b}}_3. \tag{22}$$

Substituting equation (11) into equation (22), equation (22) can be further rearranged as

$$\begin{aligned}\dot{V}_{\text{antsmc}} &= \mathbf{s}^T\left(\dot{\varepsilon} + \frac{p}{q}\boldsymbol{\Lambda}\text{diag}\left(\dot{\varepsilon}^{(p/q)-1}\right)\left(-\frac{q}{p}\boldsymbol{\Lambda}^{-1}\dot{\varepsilon}^{2-(p/q)} \quad \mathbf{M}_0^{-1}\left(-\frac{\left[\mathbf{s}^T\mathbf{W}\right]^T}{\left\|\mathbf{s}^T\mathbf{W}\right\|^2}\|\mathbf{s}\|\|\mathbf{W}\|\widehat{\Gamma}_{\text{adaptive}} + \boldsymbol{\delta}_{\text{total}}\right)\right)\right) - \frac{1}{d_1}\tilde{b}_1^T\dot{\hat{b}}_1 - \frac{1}{d_2}\tilde{b}_2^T\dot{\hat{b}}_2 - \frac{1}{d_3}\tilde{b}_3^T\dot{\hat{b}}_3 \\ &= \mathbf{s}^T\left(\frac{p}{q}\boldsymbol{\Lambda}\text{diag}\left(\dot{\varepsilon}^{(p/q)-1}\right)\mathbf{M}_0^{-1}\left(-\frac{\left[\mathbf{s}^T\mathbf{W}\right]^T}{\left\|\mathbf{s}^T\mathbf{W}\right\|^2}\|\mathbf{s}\|\|\mathbf{W}\|\widehat{\Gamma}_{\text{adaptive}} + \boldsymbol{\delta}_{\text{total}}\right)\right) - \frac{1}{d_1}\tilde{b}_1^T\dot{\hat{b}}_1 - \frac{1}{d_2}\tilde{b}_2^T\dot{\hat{b}}_2 - \frac{1}{d_3}\tilde{b}_3^T\dot{\hat{b}}_3.\end{aligned} \tag{23}$$

Substituting equation (12) into equation (23) yields

$$\begin{aligned}\dot{V}_{\text{antsmc}} &= \mathbf{s}^T\left(\frac{p}{q}\mathbf{W}\left(-\frac{\left[\mathbf{s}^T\mathbf{W}\right]^T}{\left\|\mathbf{s}^T\mathbf{W}\right\|^2}\|\mathbf{s}\|\|\mathbf{W}\|\widehat{\Gamma}_{\text{adaptive}} + \boldsymbol{\delta}_{\text{total}}\right)\right) - \frac{1}{d_1}\tilde{b}_1^T\dot{\hat{b}}_1 - \frac{1}{d_2}\tilde{b}_2^T\dot{\hat{b}}_2 - \frac{1}{d_3}\tilde{b}_3^T\dot{\hat{b}}_3 \\ &= -\frac{p}{q}\|\mathbf{s}\|\|\mathbf{W}\|\widehat{\Gamma}_{\text{adaptive}} + \frac{p}{q}\mathbf{s}^T\mathbf{W}\boldsymbol{\delta}_{\text{total}} - \frac{1}{d_1}\tilde{b}_1^T\dot{\hat{b}}_1 - \frac{1}{d_2}\tilde{b}_2^T\dot{\hat{b}}_2 - \frac{1}{d_3}\tilde{b}_3^T\dot{\hat{b}}_3.\end{aligned} \tag{24}$$

Substituting equations (14)–(16) into equation (24), equation (24) can be rewritten as

$$\begin{aligned}\dot{V}_{\text{antsmc}} &= -\frac{p}{q}\|\mathbf{s}\|\|\mathbf{W}\|\left(\widehat{\Gamma}_{\text{adaptive}} + \tilde{b}_1^{\text{T}} + \tilde{b}_2^{\text{T}}\|\mathbf{q}\| + \tilde{b}_3^{\text{T}}\|\dot{q}\|^2\right) \\ &\quad + \frac{p}{q}\mathbf{s}^{\text{T}}\mathbf{W}\boldsymbol{\delta}_{\text{total}}.\end{aligned} \tag{25}$$

Substituting equation (13) and equations (18)–(20) into equation (25) gives

$$\dot{V}_{\text{antsmc}} = -\frac{p}{q}\|\mathbf{s}\|\|\mathbf{W}\|\left(b_1 + b_2\|\mathbf{q}\| + b_3\|\dot{q}\|^2\right) + \frac{p}{q}\mathbf{s}^T\mathbf{W}\boldsymbol{\delta}_{\text{total}}. \tag{26}$$

Equation (25) can be further rearranged as

$$\dot{V}_{\text{antsmc}} \le \frac{p}{q}\|\mathbf{s}\|\|\mathbf{W}\|\left(\left\|\boldsymbol{\delta}_{\text{total}}\right\| - b_1 - b_2\|\mathbf{q}\| - b_3\|\dot{q}\|^2\right). \tag{27}$$

Therefore, $\dot{V}_{\text{antsmc}} < 0$ can be satisfied using Assumption 1. This completes the proof. □

Remark 2. The initial uncertainty upper bound of the ANSMC can be designed as a low value, and it can adaptively change based on the actual tracking errors to consider both of the tracking performance and chattering phenomenon.

Remark 3. The convergence speed of the ANSMC is mainly affected by the choice of the parameters p, q, and $\Lambda = \text{diag}[\lambda_1, \ldots, \lambda_n]$. The controller tracking performances including the accuracy and chattering are mainly designed by the choice of the parameters (b_1, b_2, b_3, $\widehat{b}_1$, $\widehat{b}_2$, and $\widehat{b}_3$ of the upper bound Γ_{constant}).

Moreover, the finite-time converge characteristic of the NTSMC has been approved for trajectory stabilization of the SISO nonlinear systems in [18]; we further extended the corresponding study to the trajectory tracking of the MIMO systems.

Equation (10) leads to

$$s_i = \varepsilon_i + \lambda_i\dot{\varepsilon}_i^{p/q}, \tag{28}$$

where $(^*)_i$ denotes the ith element of $(^*)$ and $\varepsilon_i = q_i - q_{d,i}$.

The final time $t_{s,i}$ that is taken to travel from $t_{r,i}$ to $\varepsilon_i(t_{r,i} + t_{s,i}) = 0$ for the ith element of system states can be formulated by

$$t_{s,i} = -\lambda_i^{q/p}\int_{\varepsilon_i(t_{r,i})}^{0}\varepsilon_i^{-(q/p)}\mathrm{d}\varepsilon_i = \lambda_i^{q/p}\left(\frac{p}{p-q}\right)\left|\varepsilon_{i(t_{r,i})}^{1-(q/p)}\right|, \tag{29}$$

where $t_{r,i}$ is the time when the sliding mode $s_i(t_{r,i}) = 0$ is reached.

Therefore, the convergence time for the MIMO nonlinear systems can be given by

$$t_s = \max\{t_{s,1}, \ldots, t_{s,n}\}. \tag{30}$$

This means that the system states $\mathbf{q}$ will converge to the desired $\mathbf{q}_d$ in finite time t_s after the sliding mode $\mathbf{s} = 0$ is reached.

Remark 4. To eliminate chattering, the following algorithm is introduced for the NTSMC and ANTSMC control schemes at the cost of introducing tracking errors and deteriorating the perfect stability conditions.

$$\frac{\|\mathbf{s}\|\|\mathbf{W}\|}{\|\mathbf{s}^T\mathbf{W}\|^2} = \frac{\|\mathbf{s}\|\|\mathbf{W}\|}{\left(\|\mathbf{s}^T\mathbf{W}\| + \xi\right)^2}, \tag{31}$$

where ξ is a small constant.

Remark 5. For the robot manipulator, the implementation complexity of the proposed ANSMC is mainly decided by the calculation accuracy of the estimated terms $\mathbf{M}_0$, $\mathbf{C}_0$, and $\mathbf{G}_0$. The estimated terms $\mathbf{M}_0$, $\mathbf{C}_0$, and $\mathbf{G}_0$ are calculated by the multibody dynamics of the robot manipulators. The more components of the robot manipulator are considered in the dynamic analysis of the robot system and will induce the higher implementation complexity of the proposed ANSMC controller. Generally speaking, the main components of the robot manipulator should be computed, such as the thirteen moving rigid bodies of the Stewart Platform [29]. Fortunately, the controller proposed in this paper can obtain a satisfactory performance by introducing adaptive updating laws to compensate the unmodeled dynamics influences. In practice, the calculation accuracy of the estimated terms $\mathbf{M}_0$, $\mathbf{C}_0$, and $\mathbf{G}_0$ can be chosen by comprehensively considering the difficulty of the robot multibody dynamic analysis and the implementation hardware platform capability.

5. Simulation Studies

A two-link robot manipulator is employed to evaluate the performance of the proposed ANTSMC control scheme. Its dynamic model can be formulated by equation (32) with the following parameters: r_1, r_2, J_1, J_2, m_1, and m_2 are 1 m, 0.8 m, 5 kg·m, 5 kg·m, 0.5 kg, and 1.5 kg, respectively [18].

$$\mathbf{M}_{\text{rob}}(\mathbf{q}_{\text{rob}})\ddot{q}_{\text{rob}} + \mathbf{C}_{\text{rob}}(\mathbf{q}_{\text{rob}}, \dot{q}_{\text{rob}}) + \mathbf{G}_{\text{rob}}(\mathbf{q}_{\text{rob}}) = \boldsymbol{\tau}_{\text{rob}}, \tag{32}$$

where

$$\begin{aligned}
\mathbf{q}_{\text{rob}} &= [q_1, q_2]^T,\\
M_{11} &= (m_1 + m_2)r_1^2 + m_2 r_2^2 + 2m_2 r_1 r_2 \cos(q_2) + J_1,\\
M_{12} &= M_{21} = m_2 r_2^2 + m_2 r_1 r_2 \cos(q_2),\\
M_{22} &= m_2 r_2^2 + J_2,\\
C_1 &= -m_2 r_1 r_2 \sin(q_2)\left(\dot{q}_1^2 + 2\dot{q}_1\dot{q}_2\right),\\
C_2 &= m_2 r_1 r_2 \sin(q_2)\dot{q}_2^2,\\
G_1 &= ((m_1 + m_2)r_1 \cos(q_2) + m_2 r_2 \cos(q_1 + q_2))g,\\
G_2 &= m_2 r_2 \cos(q_1 + q_2)g,
\end{aligned} \tag{33}$$

where M_{ij} denotes the (i, j) element of the matrix $\mathbf{M}_{\text{rob}}$ and C_i and G_i represent the ith elements of $\mathbf{C}_{\text{rob}}$ and $\mathbf{G}_{\text{rob}}$.

The desired trajectory $\mathbf{q}_{\text{rob},r} = [q_{1,r}, q_{2,r}]^T$ and initial trajectory $\mathbf{q}_{\text{rob},0}$ can be given by

$$\begin{aligned}
q_{1,\text{r}} = {} & a_1 \sin(\omega_1 t) + a_2 \cos(\omega_2 t) + a_3 \sin(\omega_3 t) + a_4 \cos(\omega_4 t)\\
& + a_5 \sin(\omega_5 t) + a_6 \cos(\omega_6 t),
\end{aligned} \tag{34}$$

$$\begin{aligned}
q_{2,r} = {} & b_1 \sin(\omega_1 t) + b_2 \cos(\omega_2 t) + b_3 \sin(\omega_3 t) + b_4 \cos(\omega_4 t)\\
& + b_5 \sin(\omega_5 t) + b_6 \cos(\omega_6 t),
\end{aligned} \tag{35}$$

$$\mathbf{q}_{\text{rob},0} = [1.5, -1.5]^T, \tag{36}$$

where $(a_1 \sim a_6)$, $(b_1 \sim b_6)$, and $(\omega_1 \sim \omega_6)$ are selected as (1, 1, 0.01, 1, 0.01, 0.001), (−1, −1, −0.01, −1, −0.01, −0.001), and (0.1, 0.2, 0.4, 0.8, 1.6, 3.2), respectively.

The estimated values of the dynamic parameters are assumed to be

$$\begin{aligned}
\hat{m}_1 &= 0.4\,\text{kg},\\
\hat{m}_2 &= 1.2\,\text{kg},\\
\hat{J}_1 &= 4\,\text{kg}\cdot\text{m},\\
\hat{J}_2 &= 4\,\text{kg}\cdot\text{m}.
\end{aligned} \tag{37}$$

Therefore, three controllers (NTSMC1, NTSMC2, and ANTSMC) are selected to verify the advantages of the proposed ANTSMC. To fairly compare these controllers, their control parameters except the uncertainty upper bound are chosen as the same.

$$\begin{aligned}
\boldsymbol{\Lambda} &= \begin{bmatrix} 150 & 0 \\ 0 & 150 \end{bmatrix},\\
q &= 5,\\
p &= 9,\\
\xi &= 0.001,\\
\tau_{\max} &= 40,
\end{aligned} \tag{38}$$

where $\tau_{\max}$ denotes the maximum torque of the robot manipulator.

Moreover, the appropriate constant uncertainty upper bound satisfying Assumption 1 is hard to determine in practice, especially for the existing kinds of uncertainties. Two uncertainty upper bound designs of NTSMC are selected: the lower one (NTSMC1) and the higher one (NTSMC2). Additionally, the initial value of the uncertainty upper bound of the ANTSMC is chosen as a low value, and it will adaptively adjust according to the actual tracking errors during the motion period. Therefore, the uncertainty upper bounds of the three controllers are designed as follows.

The uncertainty upper bounds of NTSMC1 are given by

$$b_1 = 1,\quad b_2 = 8,\quad b_3 = 3. \tag{39}$$

The uncertainty upper bounds of NTSMC2 are given by

$$b_1 = 10,\quad b_2 = 80,\quad b_3 = 30. \tag{40}$$

The uncertainty upper bounds of ANTSMC are given by

$$\begin{aligned} \hat{b}_{1,0} &= 1, \\ \hat{b}_{2,0} &= 1, \\ \hat{b}_{3,0} &= 1, \\ d_1 &= 5, \\ d_2 &= 0.1, \\ d_3 &= 1, \end{aligned} \tag{41}$$

where $\hat{b}_{1,0}$, $\hat{b}_{2,0}$, and $\hat{b}_{3,0}$ are the initial values of $\hat{b}_1$, $\hat{b}_2$, and $\hat{b}_3$.

5.1. Fault-Free Conditions. The numerical simulations of the robot manipulator under NTSMC1, NTSMC2, and ANTSMC are achieved in MATLAB 6.5 with the step size of 0.0005 s. The corresponding simulation results are illustrated in Figure 1, where "$q1(*)$," "$q2(*)$," "eq1 (*)," "eq2 (*)," "u1 (*)," and "u2 (*)" represent the tracking of joint 1, tracking of joint 2, tracking error of joint 1, tracking error of joint 2, control input of joint 1, and control input of joint 2 under the (*) control scheme, respectively; "q1_desired" and "q2_desired" denote the desired trajectories of joint 1 and joint 2.

The system state errors of the robot manipulator can converge to zero in finite time (2 s) under all of the three controllers, which can be observed in Figures 1(a)–1(d). However, owing to its chosen uncertainty, upper bound is lower than the actual uncertainty, and the tracking condition cannot be maintained under NTSMC1, which can be seen in 2.5~5.8 s of Figures 1(c) and 1(d). Moreover, the tracking performances of NTSMC2 and ANTSMC are satisfactory in all of the simulation time.

In the initial time, there are torque variations under the three controllers, which are always unavoidable for the mechanical systems. However, the torque command under NTSMC2 has serious chattering and saturation problems in the first 1.5 s, and there even exists slight chattering in the stabilization stage (6.7~8.7 s), shown in Figure 1(f). Besides, the torque command under NTSMC1 generates short-time chattering to compensate the tracking error in 4.9~5.2 s, which makes the tracking performance be improved after 6 s. Furthermore, the torque command under ANTSMC is always smooth in 1~20 s. Therefore, ANTSMC is the best control scheme owing to its high-accuracy tracking and smooth input command.

5.2. Faulty Conditions. To further research the influence of the unpredictable faults, the actuator faults are assumed to be

$$\delta_a = \begin{cases} 1, & t < 10, \\ 0.9 - 0.1\cos(0.1(t-10)), & t \geq 10, \end{cases} \tag{42}$$

$$\boldsymbol{\delta}_a = \operatorname{diag}(\delta_a, \delta_a), \tag{43}$$

$$\boldsymbol{\delta}_f = \begin{cases} [0 \quad 0]^T, & t < 10, \\ [-6 - 0.2\sin(0.2(t-10)) \quad -3 - 0.1\sin(0.2(t-10))]^T, & t \geq 10. \end{cases} \tag{44}$$

Besides, the parameter uncertainty, desired trajectory, and controller parameters of the robot manipulator are assumed as same as the fault-free conditions. Then, the corresponding results are presented in Figure 2.

According to equations (42)–(44), actuator faults occur after 10 s, which will cause the torque mutations under the three controllers (shown in Figures 2(e)–2(g)). Moreover, owing to the simultaneous appearances of actuator faults and disturbances, the torque command is calculated to be saturated in a short time to generate the tracking errors for the robot manipulator. After the torque saturation state, the actual trajectories will well track the desired ones under NTSMC2 and ANTSMC at the cost of short-period torque chattering, but the tracking errors will be still existing under NTSMC1.

In summary, ANTSMC is the best control scheme considering both the tracking errors and torque chattering.

6. Conclusions

In this paper, an adaptive nonsingular terminal sliding mode control (ANTSMC) scheme is proposed for the n-link robot manipulator with parameter uncertainties and actuator faults. The characteristics of the conventional nonsingular terminal sliding mode control (NTSMC) scheme, such as the global nonsingular and finite time reaching, are maintained for the proposed ANTSMC. Moreover, numerical simulations are achieved by comparing the performances of NTSMC and ANTSMC, and the advantages of ANTSMC can be summarized as follows:

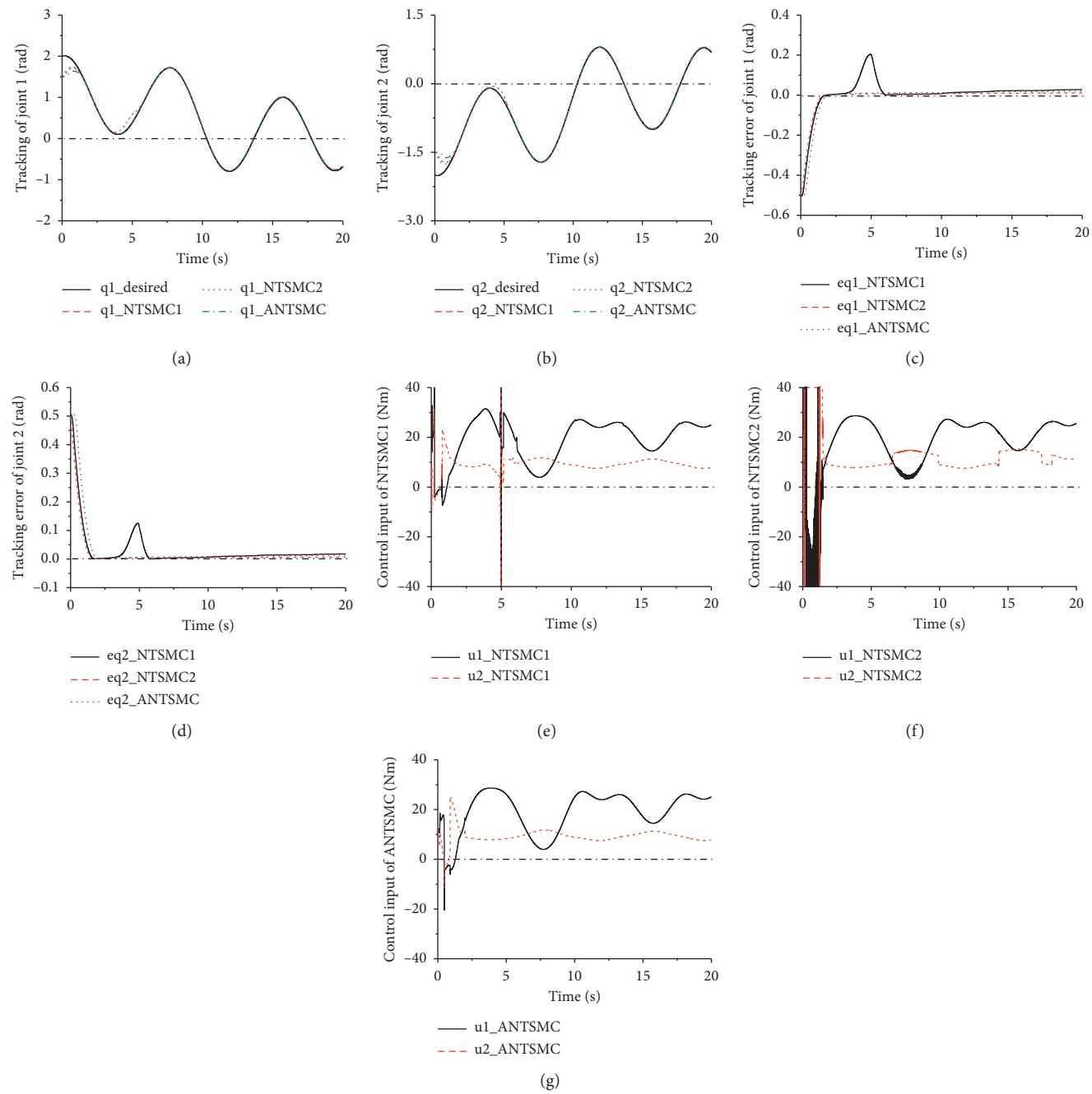

Figure 1: Fault-free condition. (a) Tracking of joint 1; (b) tracking of joint 2; (c) tracking error of joint 1; (d) tracking error of joint 2; (e) control input of NTSMC1; (f) control input of NTSMC2; (g) control input of ANTSMC.

(1) *Tracking Performance*. The actual trajectory can track the desired one under ANTSMC and NTSMC2 (higher uncertainty upper bound), even in the conditions of disturbances, faults, and saturation. However, for the trajectory under NTSMC1 (lower uncertainty upper bound), there may exist short-time or long-time errors in the fault-free and faulty conditions, respectively.

(2) *Chattering Phenomenon*. In the initial time, for the torque command under NTSMC2, there exists serious chattering and saturation problem, and the torque commands of NTSMC1 and ANTSMC are satisfactory. In the stabilization period, many factors may cause short-time chattering for the three controllers, such as large tracking error and faults occurrence.

Therefore, according to the results of the simulations, the drawback of existing tracking errors of NTSMC1, the occurrence of serious chattering and saturation for the NTSMC2, and the effectiveness of ANTSMC considering both of the trajectory performance and chattering elimination are observed, respectively.

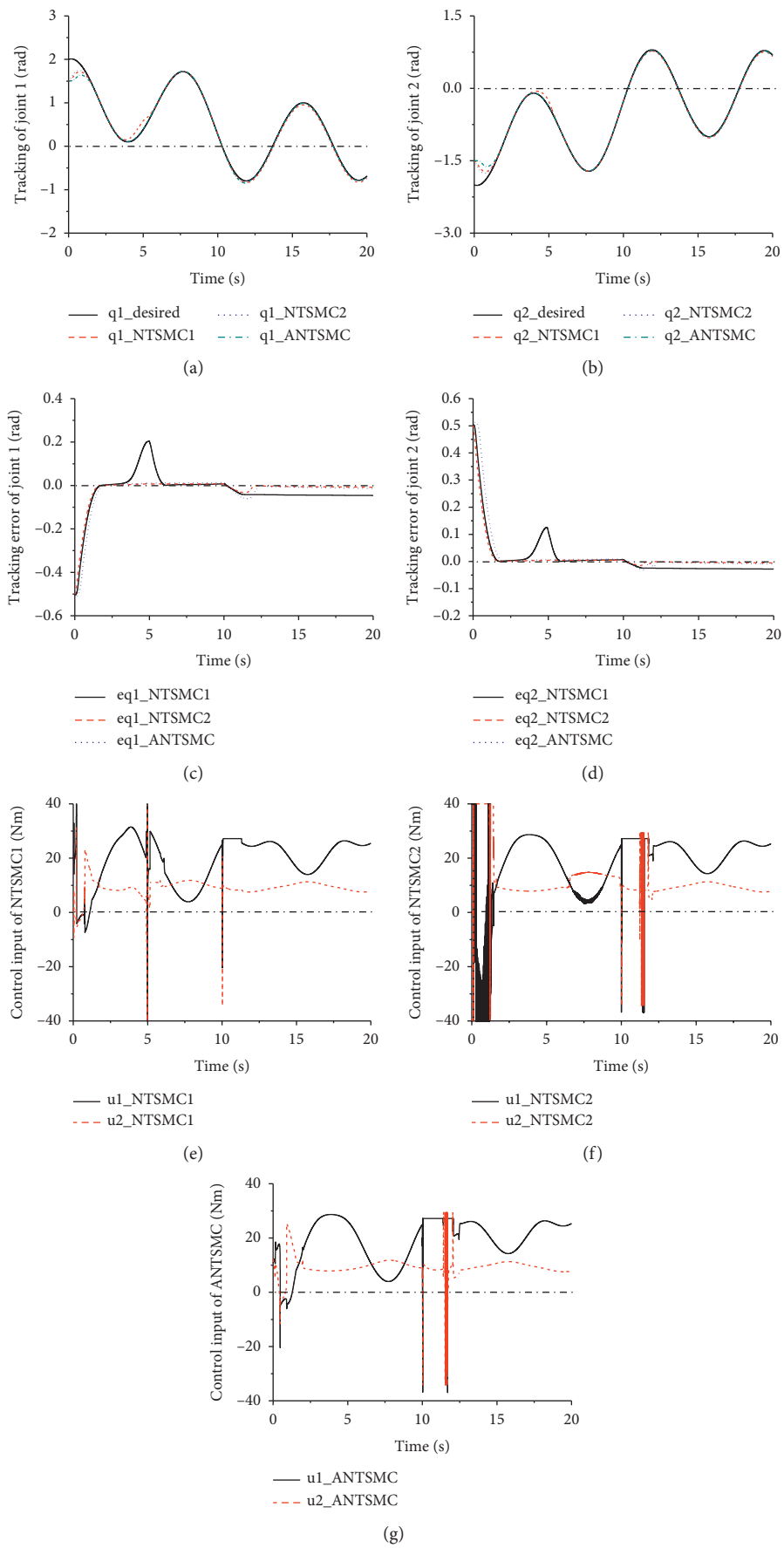

Figure 2: Faulty condition. (a) Tracking of joint 1; (b) tracking of joint 2; (c) tracking error of joint 1; (d) tracking error of joint 2; (e) control input of NTSMC1; (f) control input of NTSMC2; (g) control input of ANTSMC.

7. Future Recommendation

In this paper, we proposed an adaptive nonsingular terminal sliding mode control (ANTSMC) scheme for the general robot manipulator. Further research will be focused on the implementation to the special robot systems in practice.

Data Availability

The data used to support the findings of this study are available from the corresponding author upon request.

Conflicts of Interest

The authors declare that they have no conflicts of interest.

Acknowledgments

The authors are grateful for the financial support of this work by the National Natural Science Foundation of China (no. 51708008).

References

[1] W. E. Dixon, I. D. Walker, and D. M. Dawson, "Fault detection for robot manipulators with parametric uncertainty: a prediction-error-based approach," *IEEE Transactions on Robotics and Automation*, vol. 16, no. 6, pp. 689–699, 2000.

[2] D. Brambilla, L. M. Capisani, and A. Ferrara, "Fault detection for robot manipulators via second-order sliding modes," *IEEE Transactions on Industrial Electronics*, vol. 55, no. 11, pp. 3954–3963, 2008.

[3] M. Van, H. J. Kang, and Y. S. Suh, "A novel neural second-order sliding mode observer for robust fault diagnosis in robot manipulators," *International Journal of Precision Engineering and Manufacturing*, vol. 14, no. 3, pp. 397–406, 2013.

[4] M. L. McIntyre, W. E. Dixon, and D. M. Dawson, "Fault identification for robot manipulators," *IEEE Transactions on Robotics*, vol. 21, no. 5, pp. 1028–1034, 2005.

[5] A. H. Sabry, F. H. Nordin, A. H. Sabry, and M. Z. A. Ab Kadir, "Fault detection and diagnosis of industrial robot based on power consumption modeling," *IEEE Transactions on Industrial Electronics*, vol. 67, no. 9, pp. 7929–7940, 2020.

[6] S. M. H. Moshgani and A. Fakharian, "Fault detection and isolation for manipulator robot using optimal unknown input observer," *Control Engineering and Applied Informatics*, vol. 21, no. 3, pp. 71–79, 2019.

[7] Q. Song, W. J. Hu, L. Yin, and Y. C. Soh, "Robust adaptive dead zone technology for fault-tolerant control of robot manipulators using neural networks," *Journal of Intelligent and Robotic Systems*, vol. 33, no. 2, pp. 113–137, 2002.

[8] A. A. G. Siqueira, M. H. Terra, and C. Buosi, "Fault-tolerant robot manipulators based on output-feedback H-infinity controllers," *Robotics and Autonomous Systems*, vol. 55, no. 10, pp. 785–794, 2007.

[9] A. A. G. Siqueira and M. H. Terra, "A fault-tolerant manipulator robot based on H_2, H_∞, and mixed H_2/H_∞ markovian controls," *IEEE-ASME Transactions on Mechatronics*, vol. 14, no. 2, pp. 257–263, 2009.

[10] L. Z. Liu, L. Y. Zhang, and Y. M. Wang, "A novel robust fixed-time fault-tolerant tracking control of uncertain robot manipulators," *IET Control Theory and Applications*, vol. 15, no. 2, pp. 195–208, 2021.

[11] Y. S. Hagh, R. M. Asl, A. Fekih, H. Wu, and H. Handroos, "Active fault-tolerant control design for actuator fault mitigation in robotic manipulators," *IEEE ACCESS*, vol. 9, pp. 47912–47929, 2021.

[12] L. G. Wu, P. Shi, and H. J. Gao, "State estimation and sliding-mode control of Markovian jump singular systems," *IEEE Transactions on Automatic Control*, vol. 55, no. 5, pp. 1213–1219, 2010.

[13] Q. Meng, T. Zhang, X. Gao, and J.-Y. Song, "Adaptive sliding mode fault-tolerant control of the uncertain Stewart platform based on offline multibody dynamics," *IEEE/ASME Transactions on Mechatronics*, vol. 19, no. 3, pp. 882–894, 2014.

[14] Y. Y. Wang, X. P. Xie, M. Chadli, S. R. Xie, and Y. Peng, "Sliding mode control of fuzzy singularly perturbed descriptor systems," *IEEE Transactions on Fuzzy Systems*, p. 1, 2020.

[15] Y. Y. Wang, B. Jiang, Z. G. Wu, S. R. Xie, and Y. Peng, "Adaptive sliding mode fault-tolerant fuzzy tracking control with application to unmanned marine vehicles," *IEEE Transactions on Systems, Man, and Cybernetics: Systems*, pp. 1–10, 2020.

[16] Y. Wang, Y. Xia, H. Li, and P. Zhou, "A new integral sliding mode design method for nonlinear stochastic systems," *Automatica*, vol. 90, pp. 304–309, 2018.

[17] N. N. Shi, Z. K. Kang, Z Zhao, and Q. Meng, "Adaptive vector nonsingular terminal sliding mode control for a class of *n*-order nonlinear dynamical systems with uncertainty," *Mathematical Problems in Engineering*, vol. 2020, Article ID 7309417, 12 pages, 2020.

[18] Z. Man and X. Yu, "Terminal sliding mode control of MIMO linear systems," *IEEE Transactions on Circuits and Systems I: Fundamental Theory and Applications*, vol. 44, no. 11, pp. 1065–1070, 1997.

[19] Y. Feng, X. H. Yu, and Z. H. Man, "Non-singular terminal sliding mode control of rigid manipulators," *Automatica*, vol. 38, no. 12, pp. 2159–2167, 2002.

[20] C. K. Lin, "Nonsingular terminal sliding mode control of robot manipulators using fuzzy wavelet networks," *IEEE Transactions on Fuzzy Systems*, vol. 14, no. 6, pp. 849–859, 2006.

[21] V. Nekoukar and A. Erfanian, "Adaptive fuzzy terminal sliding mode control for a class of MIMO uncertain nonlinear systems," *Fuzzy Sets and Systems*, vol. 179, no. 1, pp. 34–49, 2011.

[22] D. Z. Xu, B. Jiang, and M. S. Qian, "Terminal sliding mode control using adaptive fuzzy-neural observer," *Mathematical Problems in Engineering*, vol. 2013, Article ID 958958, 8 pages, 2013.

[23] L. Cao, X. Q. Chen, and T. Sheng, "Fault tolerant small satellite attitude control using adaptive non-singular terminal sliding mode," *Advances in Space Research*, vol. 51, no. 12, pp. 2374–2393, 2013.

[24] H. Li, L. Dou, and Z. Su, "Adaptive nonsingular fast terminal sliding mode control for electromechanical actuator," *International Journal of Systems Science*, vol. 44, no. 3, pp. 401–415, 2013.

[25] J. Wang and Z. Sun, "6-DOF robust adaptive terminal sliding mode control for spacecraft formation flying," *ACTA Astronautica*, vol. 73, pp. 76–87, 2012.

[26] W. Q. Tang and Y. L. Cai, "High-order sliding mode control design based on adaptive terminal sliding mode," *International Journal of Robust and Nonlinear Control*, vol. 23, no. 2, pp. 149–166, 2013.

[27] J. Huang, L. N. Sun, and Z. Z. Han, "Adaptive terminal sliding mode control for nonlinear differential inclusion systems with

disturbance," *Nonlinear Dynamics*, vol. 72, no. 1-2, pp. 221–228, 2013.

[28] M. Jin, J. Lee, and P. Chang, "Practical nonsingular terminal sliding-mode control of robot manipulators for high-accuracy tracking control," *IEEE Transactions on Industrial Electronics*, vol. 56, no. 9, pp. 3593–3601, 2009.

[29] Q. Meng, T. Zhang, J.-F. He, J.-Y. Song, and J.-W. Han, "Dynamic modeling of a 6-degree-of-freedom Stewart platform driven by a permanent magnet synchronous motor," *Journal of Zhejiang University Science C*, vol. 11, no. 10, pp. 751–761, 2010.